Simultaneous imaging and inversion with the inverse scattering series

Kristopher A. Innanen (University of British Columbia) and Arthur B. Weglein (University of Houston)

Abstract

The inverse scattering series holds the promise of precise reflector location (imaging) and target identification (inversion proper) in multiple dimensions and in the absence of complete knowledge of the medium wavespeed structure. In this article we show, using the theoretical milieu of a layered acoustic medium and normal incidence wave field, that much of that portion of the series which concerns itself with tasks of *imaging* and *inversion* of seismic primaries is captured by a simple set of nonlinear operations carried out upon the integral of the Born approximation. This simultaneous imaging and inversion formula is shown to capture aspects of both the imaging and inversion subseries of the inverse series entire. The formula, whose n'th term involves the n'th derivative of the n'th power of the input, is tested numerically. We demonstrate the use of a simple regularization of the derivative operators, which stabilizes the computation and permits the reconstruction of models of varying contrasts, using data with small amounts of incoherent noise. We comment on the behaviour of the formula from a signal processing standpoint, and speculate on the possible nature of a multidimensional incarnation of this approach.

Introduction

The inverse scattering series is pursued as a means to process and invert seismic data for the simple reason that it is the only known method for multidimensional direct inversion. However, its superficial promise of "black-box" like transformation of the data into the model has not been realized, because of (numerical) divergence for all but the lowest-contrast examples (Carvalho, 1992). Experience and empiricism have shown that the utilization of the inverse scattering series requires an almost term-by-term understanding of its behaviour, and an informed use of the data operations it espouses. The idea of task-separation has been the critical conceptual leap in the success of the inverse scattering series to date (Weglein et al., 1997, 2003). The tasks are fourfold: (*i*) removal of free-surface multiples, (*ii*) attenuation of internal multiples, (*iii*) imaging of primaries (reflector location), and (*iv*) inversion of primaries (target identification). In this research we concern ourselves with the latter two tasks. Candidate subseries which are involved with the distinct and separate tasks of imaging and medium parameter inversion have been identified and are the subject of intensive research at present. Both methods are considered to act upon data which are made up of primaries only – it is assumed that all multiples are removed. This is characteristic of the task separation approach: a processing step is accomplished, and then the problem is recast as if the previous task (e.g. multiple elimination) never existed. Amongst other recent advances, the form of the n'th term of a leading-order imaging subseries (task *iii*) has been shown numerically to locate reflectors without knowledge of the medium wavespeed (Shaw et al., 2003) for 1D normal incidence cases; furthermore, the second term in the inversion subseries (task *iv*) has been shown to improve the estimation of density and bulk modulus beyond the linearized form for a 1D case with offset (Weglein et al., 2003). Hence, early evidence is strongly suggestive of the practical value of task separation in the latter tasks.

Nevertheless, there is no absolute indication that the separation of imaging and inversion tasks is a requisite step. That is a strong theme in this article: we note that with certain approximations, combinations of terms can result in forms that are simply computable and readily stabilized numerically, and which amount to simultaneous imaging and inversion of the input data. It seems imprudent at present to say that separating or combining these tasks is in all ways the superior approach: we are satisfied to investigate all avenues.

After briefly reviewing theory and quoting the mathematical form of two subseries currently under study by others, we introduce a form for the simultaneous imaging and inversion of seismic data. We show its partial inversion and imaging nature, by expanding the formula for several orders and contrasting this expansion with existing subseries; we comment on the meaning of "partial". We propose an *ad hoc* regularization or stabilization of the formula and demonstrate its numerical implementation using models with varying levels of complexity, magnitudes of contrast, and data noise. Finally, we analyse the formula from a signal processing viewpoint, to develop an understanding of what a formula which concurrently locates and identifies medium contrasts *does* to the input data. The work discussed here is also developed and discussed in Innanen (2003).

The inverse scattering series is based on two wave-theoretic relationships, between reference and non-reference wave operators and Green's operators. Following (Weglein et al., 2003), these are:

$$L_0 G_0 = -\delta(r - r_s), \quad LG = -\delta(r - r_s) \qquad (1)$$

respectively. For instance, in a 1D normal incidence acoustic medium in the space-frequency domain, we have

$$L_0 = \frac{d^2}{dz^2} + \frac{\omega^2}{c_0^2}, \quad L = \frac{d^2}{dz^2} + \frac{\omega^2}{c^2(z)}. \tag{2}$$

A perturbation operator is defined as

$$V = L - L_0 = k^2 \alpha(z), \tag{3}$$

where $\alpha(z)=1-c_0^2/c^2(z)$ and $k=\omega/c_0$. The scattering equation, or Lippmann-Schwinger equation, is expanded in terms of $\boldsymbol{V}$ and $\boldsymbol{G_0}$ to produce an expression for the wave field $\boldsymbol{G}$. This is the Born series:

$$G = G_0 + G_0 V G_0 + G_0 V G_0 V G_0 + \ldots \tag{4}$$

It is inverted by setting $\boldsymbol{V=V_1+V_2+V_3+\ldots}$, inserting this into (4), and equating like orders. Considering the data to be the scattered field $\boldsymbol{D=\psi_s=G-G_0}$, and considering incident plane wave fields $\boldsymbol{\psi_0}$ for the 1D normal incidence case this amounts to

$$\psi_s = G_0 V_1 \psi_0, \tag{5}$$

$$0 = G_0 V_2 \psi_0 + G_0 V_1 G_0 V_1 \psi_0, \tag{6}$$

etc., where each term has been projected onto the measurement surface. These equations are solved sequentially, order by order. Using a homogeneous acoustic Green's function and the perturbation operator in (3), the orders $\boldsymbol{V_n}$ may be written in terms of $\boldsymbol{\alpha_n}$, and the higher order terms may be cast in terms of the Born approximation $\boldsymbol{\alpha_1}$. Up to second order, this is:

$$\alpha_1(z) = 4\int_0^z D(z')dz', \text{ and} \tag{7}$$

$$\alpha_2(z) = -\frac{1}{2}\alpha_1^2(z) - \frac{1}{2}\left[\frac{d\alpha_1}{dz}\right]\int_0^z \alpha_1(z')dz'. \tag{8}$$

As low as second order, i.e. (8), some basic forms are established which remain throughout the series when it is cast in this way. Namely, the higher order terms tend to involve weighted (*i*) powers, (*ii*) integrals, and/or (*iii*) derivatives of the Born approximation. Terms in powers of $\boldsymbol{\alpha_1}$ alone are associated with the inversion task, and many terms which involve integro-differential operations are associated with the imaging task. Specifically, we quote the form of the inversion subseries for this simple physical configuration:

$$\alpha_{INV}(z) = \sum_{j=1}^{\infty} \frac{(-1)^{j-1} j}{4^{j-1}} \alpha_1^j(z). \tag{9}$$

For a 1D normal incidence experiment over a single interface with the reflection coefficient $\boldsymbol{R_1}$, we have $\boldsymbol{\alpha_1}=4R_1$, and hence

$$\alpha_{INV}(z) = 4R_1 - 8R_1^2 + \ldots \tag{10}$$

Also, the form of the leading order imaging subseries of Shaw et al. (2003):

$$\alpha_{LI}(z) = \sum_{j=0}^{\infty} \frac{(-1/2)^j}{j!} \left[\frac{d^j \alpha_1}{dz^j}\right]\left(\int_0^z \alpha_1(z')dz'\right)^j. \tag{11}$$

These subseries are concerned with, respectively, correction of the amplitudes of the Born approximation, and correction of the location of the discontinuities of the Born approximation.

Simultaneous Imaging and Inversion

In this section we present an expression which, in implementing a combination of weighted powers of, and integral and differential operations on, the Born approximation, is intimately connected to tasks of both imaging and inversion. Consider the expression:

$$\alpha_{SII}(z) = \sum_{j=1}^{\infty} K_j \frac{d^j}{dz^j}\left(\int_0^z \alpha_1(z')dz'\right)^j, \tag{12}$$

where

$$K_j = \frac{(-1)^{j-1}}{j 2^{2(j-1)}}\left(\sum_{k=0}^{j-1} \frac{1}{k!(j-k-1)!}\right). \tag{13}$$

Expanding this expression for several orders produces terms, some of which may be grouped as

$$\alpha_1 - \frac{1}{2}\alpha_1^2 + \frac{1}{4}\alpha_1^3 - \frac{1}{8}\alpha_1^4 + \ldots, \quad \text{or as} \tag{14}$$

$$\alpha_1 - \frac{1}{2}\frac{d\alpha_1}{dz}\int_0^z \alpha_1(z')dz' + \frac{1}{8}\frac{d^2\alpha_1}{dz^2}\left(\int_0^z \alpha_1(z')dz'\right)^2 - \ldots \tag{15}$$

The first set of terms matches the inversion subseries (9) up to second order and then diverges from it; we interpret this as a partial inversion subseries, which is accurate at reflection coefficients empirically determined to be below ~0.4. The second set of terms reproduces exactly the leading order imaging subseries. In other words, this expression implicitly includes terms that are concerned with reflector location and target identification. We expect that (12) should be observed to correct both the amplitude and location of the Born approximate contrasts.

Computational Issues

Assuming the data associated with a 1D normal incidence experiment are a sequence of weighted, delta-like discontinuities, the integral of the Born approximation (which is in essence the second integral of the data) will be a piecewise linear signal, with its linear elements discontinuously conjoining at the "Born depths". Clearly to compute (12) numerically we must (*i*) exponentiate this signal, and then (*ii*) take the derivative of the result. Anticipating some level of instability, for numeric implementation we propose approximating the derivative operators in the Fourier domain with a smoothed window that flexibly truncates the higher frequencies. This

regularization procedure is to be governed by the width of the window, which should be widened and shrunk depending on the contrasts and noise level.

Numerical Examples

Figure 1 illustrates the form of the synthetic input to (12) used in the demonstrations of this article. Figure 1a is the form of the data, weighted impulses, delayed according to the depths characterizing a layered acoustic model (with piecewise constant wavespeeds c_0, c_1, c_2, etc. Figure 1b is the Born approximation to the perturbation, i.e. α_1; it contains errors in amplitude and location that grow with the model contrasts. Finally, Figure 1c is the integral of the Born approximation of 1b; this piecewise linear signal typifies the input to the terms of the imaging and inversion procedure implied by (12). The model used to create this data is in Table 1; this same table details all the models used in the forthcoming examples.

Depths (m)	Model 1 (m/s)	Model 2 (m/s)	Model 3 (m/s)
300-500	1600	1600	2000
500-700	1650	1650	2200
700-750	1467	1600	1423
750-800	-	1570	-
800-870	-	1530	-
870-910	-	1500	-
910-∞	-	1454	-

Table 1. Depths and wavespeeds of stratified acoustic models used in numerical examples. The bottom wavespeed is chosen in each case such that the end of the signal does not act like a strong reflector. All examples have a reference wavespeed of c_0 = 1500 m/s at depths < 300m.

Figures 2—4 contain the results of the imaging/inversion procedure. The figures are similarly organized: the top panel (a) is the data plotted against pseudo-depth z. The second panel (b) compares the computed Born approximation (dashed) against the true perturbation (dotted); to add value, the imaging and inversion must correct the former such that it resembles the latter. The third panel (c) compares the Born approximation (dashed) against the correction produced by ~100 terms computed using (12). The bottom panel (d) compares the sum of the Born approximation and the correction (solid) against the true perturbation (dotted).

In Figure 2 the constructed model (although slightly low-pass filtered by the derivative-stabilization procedure) is visually very close to the true perturbations. At these contrast levels (see Table 1, Model 1), the simultaneous imaging and inversion formula is capturing all the requisite structure and amplitudes.

In Figure 3 we present an example of a model construction in which the data, associated with Model 2, is corrupted by ~%1 Gaussian noise. While the small amount of noise clearly disrupts the quality of the result, the results are encouraging in that data error does not prove "fatal" to the procedure. We surmise that the fidelity of the Born approximation is of importance to the inversion via this type of inverse scattering series methodology.

Finally, in Figure 4 (Model 3), the large contrast case, in addition to an increased level of derivative smoothing, a clear discrepancy still exists between the constructed model (Figure 4d, solid) and the true perturbation (dotted). We interpret this as being due to missing higher order imaging subseries terms, which are not captured by (12). Nevertheless, the constructed model is clearly an improvement on the Born approximation for these high contrast examples.

A Signal Processing View

The key in this article is not to espouse a new method for 1D normal incidence inversion. Rather, we report on an ongoing campaign to understand the workings of the series, and to use it as a means by which to generate algorithms for the inversion of seismic data for multidimensional, multiparamter media. The extension of the imaging/inversion procedure of (12) to multiple dimensions, by no means an immediate or trivial task, is at present being addressed. Existing inverse scattering-based processing algorithms share, from 1D to 3D, basic underlying signal processing tasks: for instance, the prediction of free-surface multiples involves data autoconvolution regardless of the dimension of the problem. Hence we might hope to anticipate cross-dimensional features of a simultaneous imaging/inversion algorithm by analysing the basic mechanisms of (12).

The engine of this procedure is the operator

$$\frac{d^n}{dz^n}(\cdot)^n, \tag{16}$$

i.e. the n'th derivative of the n'th power of the input. The input, meanwhile, is assumed to be a piecewise linear signal. Away from its discontinuities, therefore, a general input may be written as $H(z)=az+b$. (Notice that if the model is a single interface, with reflection coefficient R_1, then $a=4R_1$ and $b=0$.) Applying (12) to this input produces, for the first few terms, and including the single interface example,

$$K_1 \frac{d}{dz} H(z) = a = 4R_1, \tag{17}$$

$$K_2 \frac{d^2}{dz^2} H(z) = -\frac{1}{2}a^2 = -8R_1^2, \ \ldots \tag{18}$$

Away from the discontinuities, therefore, (12) operates quite gently on the input signal – in fact, it enacts the transformation from a linear function to a constant function with specific weights. By comparing the rightmost terms in (17) and (18), with the inversion subseries of (10), we see that these weights ensure that the output corresponds to that required by the inversion subseries (or parts thereof). Hence, away from discontinuities, (12) behaves like the inversion subseries. The operator (16) is also an edge detector, however: the

"gentle" behaviour above only holds around portions of the signal that resemble low-order polynomials. Figure 5 illustrates the behaviour of (16) near the characteristic discontinuity of a piecewise linear signal for the orders 1—4. Numerically, the exponentiation acts to increase the amplitude of the derivatives of the discontinuity in a specific way; the derivatives themselves appear to by and large keep their recognizable shapes. The leading order imaging subseries is characterized by just such weighted derivatives of increasing order; in other words, at and near the discontinuities of the input, (12) acts like the leading order imaging subseries.

To summarize, the expression (12) is a flexible operator which scans the integral of the Born approximation for discontinuities, invoking a partial inversion subseries-like operation away from them, and a leading-order imaging subseries-like operation near them.

Conclusions

In the simple physical framework of a 1D constant density acoustic medium, the inverse scattering series may be cast such that it involves repeated exponentiation, integration, and differentiation of the Born approximation. The patterns that result are such that a simple, computable formula reproduces many of the terms identified with the imaging and inversion of primaries. The formula is readily shown to produce good quality results on 1D synthetic data, if the derivative operators are truncated at the highest frequencies. The main goal for future research is to generalize these investigations to 2D and 3D. To at least conceptually broach this issue, we include an analysis of the behaviour of the formula in the signal processing sense, i.e. determine what it does, as an operator, to the input signal. The results suggest that the method distinguishes between what might be termed "quiescent" regions of the data and "active" regions of the data; in other words, the inversion component of the operator dominates where there are no discontinuities in the integrals of the data, whereas the imaging component dominates where the singular events of the seismic experiment occur. We speculate that algorithms in higher dimensions, if achievable, may share these traits.

Acknowledgments

We thank the sponsors of M-OSRP and CDSST, and the valuable comments and suggestions of Simon Shaw, Ken Matson, and Tad Ulrych.

References

Carvalho, P. M., *Free-surface Multiple Elimination Method Based on Nonlinear Inversion of Seismic Data*, 1992. Ph.D Thesis, Universidade Federal da Bahia, Brazil (in Portuguese).

Innanen, K. A., *Methods for the Treatment of Acoustic and Absorptive/Dispersive Wave Field Measurements*, 2003. Ph.D Thesis, University of British Columbia, Canada.

Shaw, S. A., A. B. Weglein, D. J. Foster, K. H. Matson and R. G. Keys, *Isolation of a Leading Order Depth Imaging Series and Analysis of its Convergence Properties*, 2003. In Preparation.

Weglein, A. B., F. A. Gasparotto, P. M. Carvalho and R. H. Stolt, *An Inverse Scattering Series Method for Attenuating Multiples in Seismic Reflection Data*, 1997. Geophysics **62**, 1975--1989.

Weglein, A. B., F. V. Araujo, P. M. Carvalho, R. H. Stolt, K. H. Matson, R. Coates, D. J. Foster, S. A. Shaw, and H. Zhang, *Topical Review: Inverse-scattering Series and Seismic Exploration*, 2003. Inverse Problems, to appear.

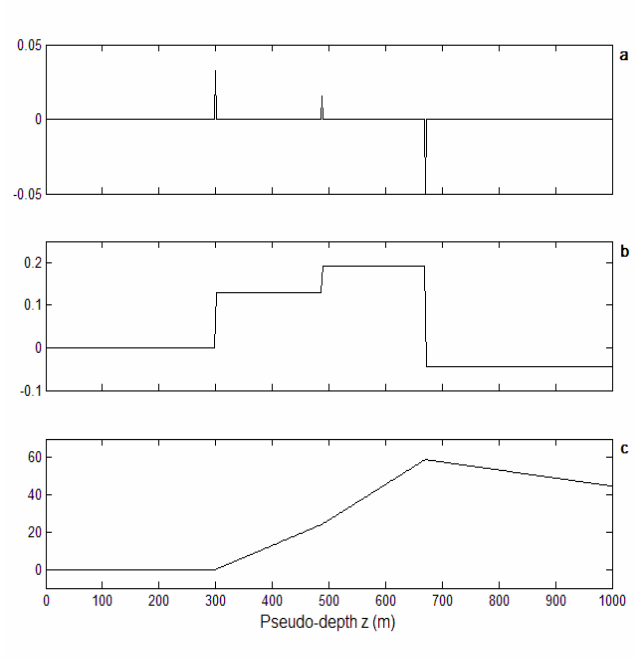

Figure 1. Synthetic data and inputs to the imaging/inversion procedure: (a) data associated with model 1, (b) Born approximation to the perturbation, computed via Fig. 1a and the reference wavespeed c_0, (c) the integral of the Born approximation, i.e. the input used in (12). All plots are against pseudo-depth z (m).

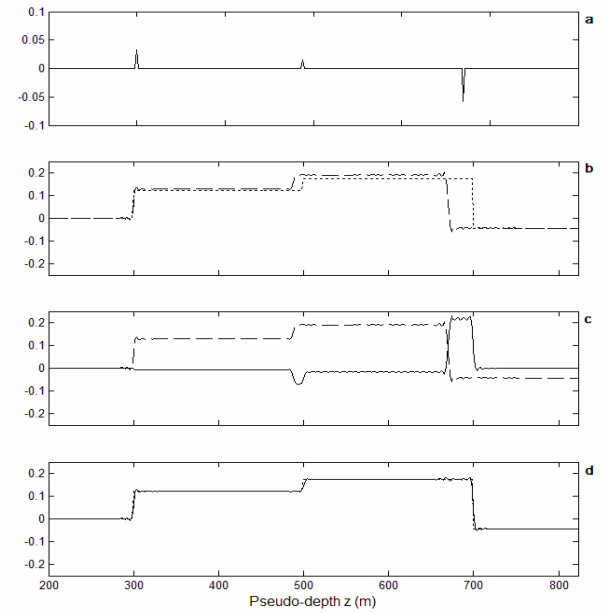

Figure 2. Imaging/inversion results for model 1; all plots are against pseudo-depth z (m). (a) Data, (b) Born approximation and true perturbation, (c) Born approx. and correction from (12), (d) Constructed perturbation vs. true perturbation.

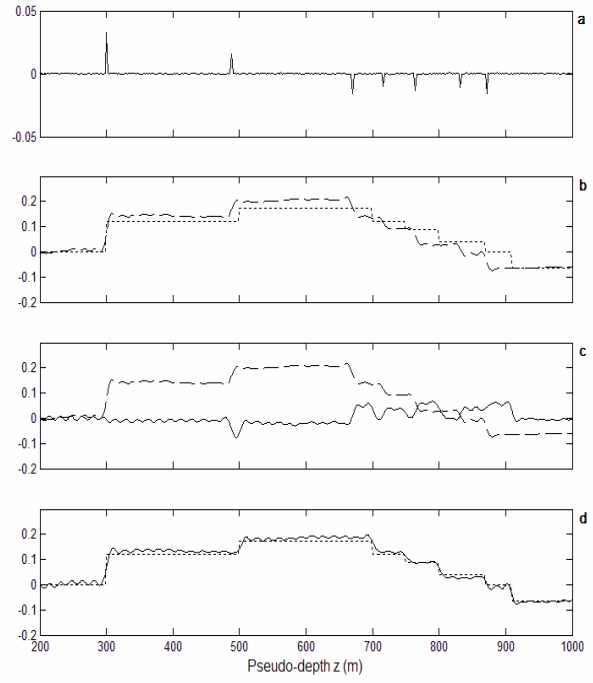

Figure 3. Imaging/inversion results for model 2 + %1 Gaussian noise; all plots are against pseudo-depth z (m). (a) Data, (b) Born approximation and true perturbation, (c) Born approx. and correction from (12), (d) Constructed perturbation vs. true perturbation.

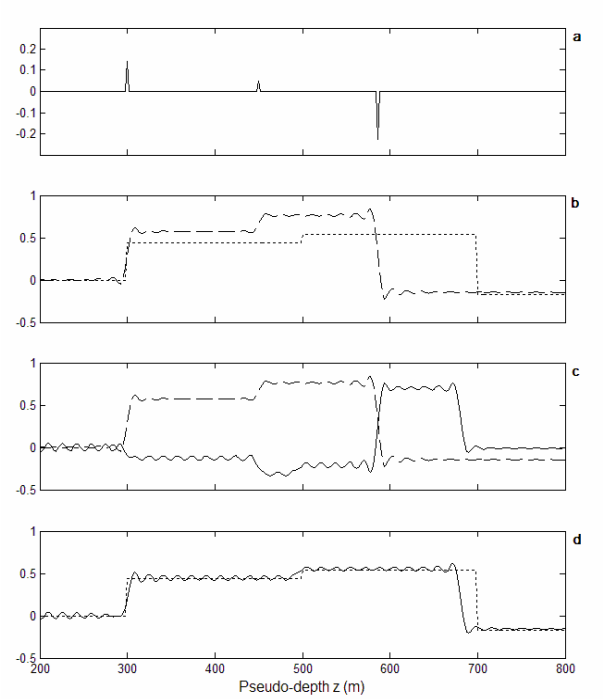

Figure 4. Imaging/inversion results for model 3 (high contrast); all plots are against pseudo-depth z (m). (a) Data, (b) Born approximation and true perturbation, (c) Born approx. and correction from (12), (d) Constructed perturbation vs. true perturbation.

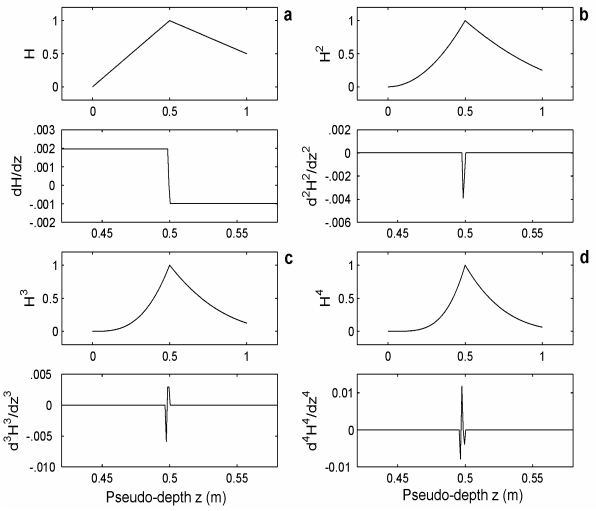

Figure 5. Plots of low powers of a piecewise linear signal (a—d, top panels) and their respective derivatives as per (12) (a—d, bottom panels). The general piecewise linear signal is denoted H. All plots are against pseudo-depth z (m).